Atlas-Based Segmentation of Neck Muscles from MRI for The Characterisation of Whiplash Associated Disorder

Abdulla Al Suman[1], Mst. Nargis Aktar[1], Md. Asikuzzaman[1], Alexandra Louise Webb[2], Diana M. Perriman[2, 3], and Mark R. Pickering[1]
[1] School of Engineering and Information Technology
The University of New South Wales, Canberra, Australia
[2] Medical School, Australian National University, Canberra, Australia
[3] Trauma and Orthopaedic Research Unit, Canberra Hospital, Canberra, Australia

ABSTRACT

Whiplash-associated disorder (WAD) is a commonly occurring injury that often results from neck trauma suffered in car accidents. However the cause of the condition is still unknown and there is no definitive clinical test for the presence of the condition. Researchers have begun to analyze the size of neck muscles and the presence of fatty infiltrates to help understand WAD. However this analysis requires a high precision delineation of neck muscles which is very challenging due to a lack of distinctive features in neck magnetic resonance imaging (MRI). This paper presents a novel atlas-based neck muscle segmentation method which employs discrete cosine-based elastic registration with affine initialization. Our algorithm shows promising results based on clinical data with an average Dice similarity coefficient (DSC) of 0.84±0.0004.

Keywords: Atlas, registration, Dice similarity coefficient, affine, elastic motion model.

1. INTRODUCTION

Sudden forward and backward movement of the head and neck can often cause injury to the neck muscles which may lead to chronic neck pain. This condition is known as whiplash associated disorder (WAD). WAD is the major source of claims for traffic-related damages [1]. In the Western world, almost one in 1000 residents suffer neck trauma and 100 in 1000 of these neck-trauma patients will go on to suffer from WAD [2]. This results in a significant cost to society [3]. The cross-sectional area (CSA) of neck muscles and levels of intra-muscular fat have been shown to vary in patients with WAD when compared to healthy individuals [4]. Researchers have begun to analyze the size of neck muscles and the presence of fatty infiltrates in order to better understand WAD [4]. However this analysis requires a high-precision delineation of neck muscles which is very challenging because of the difficulty with detecting the muscle outlines on neck MRI.

Although manual delineation has been used in prior studies, it is time-consuming and tedious and also suffers from the problem of inter- and intra-observer variations [6]. Therefore, it is not well suited in statistical analysis and patient follow-up procedures [5]. Alternatively, automatic delineation does not have these drawbacks but has the problems of accuracy due to the following issues associated with neck MRI images: The anatomy of the neck muscles is very complex with many muscles of similar intensity and texture sharing a compact space. The boundaries of some muscles are also not clear due to the problems of imaging artifacts such as partial volume effect, low contrast and inhomogeneity. Intramuscular fat can also generate false boundaries. The anatomical variability among individuals also hinders the accurate segmentation of neck muscles [6]. To the best of our knowledge, no work on automatic neck muscle segmentation has been proposed in the currently available literature. However, some segmentation work has been conducted on other muscles of the human body such as the leg, pectoral region and tongue [6–13].

Algorithms for the segmentation of leg muscles have been proposed in [6–9]. Andrews *et al*. in [6] demonstrated a globally minimized probabilistic segmentation approach using a generalized log-ratio-based shape model with pre-segmentation of fat, bone and muscle classes. Baudin *et al*. in [7] proposed a procedure for automatic voxels detection inside muscles using a border graph designed from local intensity variances and obtained good results using these voxels as seeds for subsequent segmentation. However, it may be difficult to ensure that these seeds reside within the inside of a muscle region. Essafi *et al*. in [8] employed wavelets for representing shape variation of calf muscles. This method

Eighth International Conference on Digital Image Processing (ICDIP 2016), edited by Charles M. Falco, Xudong Jiang
Proc. of SPIE Vol. 10033, 100334L · © 2016 SPIE · CCC code: 0277-786X/16/$18 · doi: 10.1117/12.2243754

depends on matching explicit face profiles to muscle boundaries and can experience difficulty in detecting false boundaries. Wang *et al*. in [9] implemented an iterative corrective learning method by combining corrective learning with an auto-context learning model for canine leg muscle segmentation.

Pectoral muscle segmentation in breast MRI and mammography was considered in [10–12]. Ganesan *et al*. in [10] provided a review of research papers on pectoral muscle segmentation. Gubern-Mérida *et al*. in [11] studied the performance and complexity between a multi-atlas and probabilistic model-based pectoral muscle segmentation. Kwok *et al*. in [12] proposed an adaptive algorithm for automatically extracting the pectoral muscle from digitized mammograms by estimating the contour using a straight line approximation on a mediolateral oblique view.

Ibragimov *et al*. in [13] introduced a method for segmenting tongue muscles from super-resolution MRI images by applying a landmark-based game-theoretic framework.

These previously proposed methods are not applicable to neck muscle segmentation due to its complex anatomy and confounding imaging artifacts. Of the automatic segmentation methods available, atlas-based methods are promising as they can simultaneously segment several structures while preserving anatomical topology. However, the accuracy of atlas-based segmentation depends mainly on image registration. In this work, an atlas-based neck muscle segmentation approach based on a framework of registration algorithms is proposed. Initially, MRI volumes are registered using an affine registration with a similarity transformation-based initialization. It uses the sum-of-conditional variance with partial volume interpolation (SCVPVI) as the similarity measure and Gauss-Newton gradient descent optimization. Then, these volumes are registered again slice-by-slice using an elastic motion model in three global steps, with different motion parameters, and one local step which is the main novelty of this paper. Finally, the labels from the atlas are transferred onto the test MRI volume.

2. PROPOSED METHOD

In our approach, we use a hierarchical atlas registration framework consisting of five steps to align the atlas and test MRI volume to be segmented. The first step uses a linear affine registration and the remaining four a nonlinear elastic registration. Then, the atlas labels are mapped onto the test MRI image using the registered parameters. The output of each step is used as the input to the next step. The affine registration step uses SCVPVI as the image-matching metric. The elastic registration step exploits the sum-of-conditional variance (SCV) as the similarity measure. In the following subsections, we present these registration algorithms using $I(x, y, z)$ and $I'(x', y', z')$ as the test and atlas images respectively.

2.1 Sum-of-Conditional Variance with Partial Volume Interpolation (SCVPVI)-based Affine Registration

A linear affine transformation with 12 parameters is used to correct global mismatches in position and orientation between the atlas and test volumes. Gradient-based Gauss-Newton optimization is used to optimize the spatial transformation parameters. The SCVPVI measure, which was recently proposed for registering multi modal images, is used as the similarity measure [14]. The non-rigid geometrical transformation model between the atlas and test volume images is defined as [14]:

$$\begin{aligned} x' &= e_0 + e_1 x + e_2 y + e_3 z \\ y' &= f_0 + f_1 x + f_2 y + f_3 z \\ z' &= g_0 + g_1 x + g_2 y + g_3 z \end{aligned} \tag{1}$$

Where $e_0, e_1, e_2, e_3, f_0, f_1, f_2, f_3, g_0, g_1, g_2, g_3$ are the spatial parameters.

2.2 Discrete Cosine-based Nonlinear Elastic Registration

The volume obtained from affine registration is registered again slice-wise using the non-linear discrete cosine transformation. It uses eight transform parameters for the further correction of global mismatches in position and orientation between the atlas and test volumes in the first step. We repeat this procedure with 18 and 32 transform parameters using the previous registration step's output as input to the current registration step in the second and third

steps respectively. Then, each slice of the volumes registered using 32 motion parameters is partitioned into four blocks for applying local elastic registration which is applied block-wise using 18 motion parameters. Gradient-based Gauss-Newton optimization is used to optimize the spatial transformation parameters for all the registration steps. The test image $I(x, y)$ and atlas image $I'(x', y')$ are related by a coordinate transformation of the form [15]:

$$x_i' = x_i + \sum_{k=1}^{P/2} m_k \varphi_k (x_i y_i)$$
$$y_i' = y_i + \sum_{k=P/2+1}^{P} m_k \varphi_k (x_i y_i) \quad (2)$$

Where m_k are the transform parameters, φ_k are the basis functions and P is the number of parameters.

Discrete cosines are used as the basis functions to estimate variability between patients, with those of the geometrical transformation given by [15]:

$$\varphi_k (x_i, y_i) = \varphi_{k+P/2} (x_i, y_i) = \cos\left(\frac{(2x_i + 1)\pi u}{2M} \right) \cos\left(\frac{(2y_i + 1)\pi u}{2N} \right) \quad (3)$$

(3) Where $k = su + v + 1; u, v = 0,1,2,\cdots, s-1; s = \sqrt{\frac{P}{2}}$; and M and N are the horizontal and vertical dimensions of an image to be registered respectively.

3. NUMERICAL RESULTS AND DISCUSSION

Our experiments were conducted on a HP z230 tower workstation with an Intel(R) Core(TM) i7-4770 CPU, 3.40 GHz processor and 4 GB RAM running Windows 7 SP1 operating system. In our experiment, clinical neck MR images of 7 patients of males and females with age ranges from 22 to 34 years were captured by the Canberra Imaging Group at Calvary John James Hospital, Deakin, Canberra, Australia using a 3-Tesla Skyra scanner (Siemens, Erlangen, Germany). The data set has 3 healthy and 4 acute whiplash subjects. Each patient's data contains 256 × 256 × 45 neck images with voxel sizes around 0.8594×0.8594×4mm^3. Manual delineation by an expert of the sternocleidomastoid, obliquus capitus inferior, semispinalis capitis and splenius capitis muscles in the volume images were performed to obtain the ground truth and atlas volume against which the auto-segmentation results were validated because normally the cross sectional area of these muscles changes due to WAD [4]. This data set is very challenging in terms of muscle segmentation because of the large anatomical shape variations due to the weight differences among the patients, image inhomogeneity, low contrast, similar intensities and textures of muscles, and presence of intra- and inter-muscular fat.

The leave-one-out technique was used to validate our method: for each person, the remaining 6 individuals are regarded as possible atlases. The automatic segmentation results for four neck muscles obtained from one of the test MRI volume images using a single optimal atlas are shown in Fig. 1. As can be seen, they match fairly well with those from manual segmentation. The automatic and manual segmentations were compared in a slice-wise manner for the C1-C7 intervertebral levels considered as the region of interest (ROI) for WAD [4] to calculate the mean DSC for each muscle in each patient. The average DSC values over 7 patients with variance for the four muscles are tabulated in Table 1, with those for symmetrical structures averaged due to lack of space. We note that the splenius capitis muscle has a relatively low mean DSC due to the existence of high gradient magnitudes of other muscles nearby. As the average DSC for the four muscles is 0.84, our algorithm provides quite accurate muscle segmentation. This DSC value compares favourably with those reported from other methods in the human muscle segmentation literature [6,8,9,11,13] as shown in Table 2. Only Ibragimov *et al*. in [13], who used super-resolution MR images, obtained similar accuracy. Andrews *et al*. in [6] also found almost similar results for probabilistic segmentation. However, as the anatomical complexity of neck muscles is greater than those of the thigh, tongue and pectoral muscles due to their large number and higher proximity, our method demonstrates promising results for muscle segmentation. Physician can observe the existence of pathology by observing the 3D view of the segmented muscles as CSA changes due to WAD.

Muscle Name	DSC
Sternocleidomastoid	0.83±0.0002
Semispinalis capitis	0.85±0.0005
Splenius capitis	0.82±0.00002
Obliquus capitus inferior	0.87±0.001

Table 1. Mean DSC values for four neck muscles over 7 subjects for C1-C7 intervertebral levels.

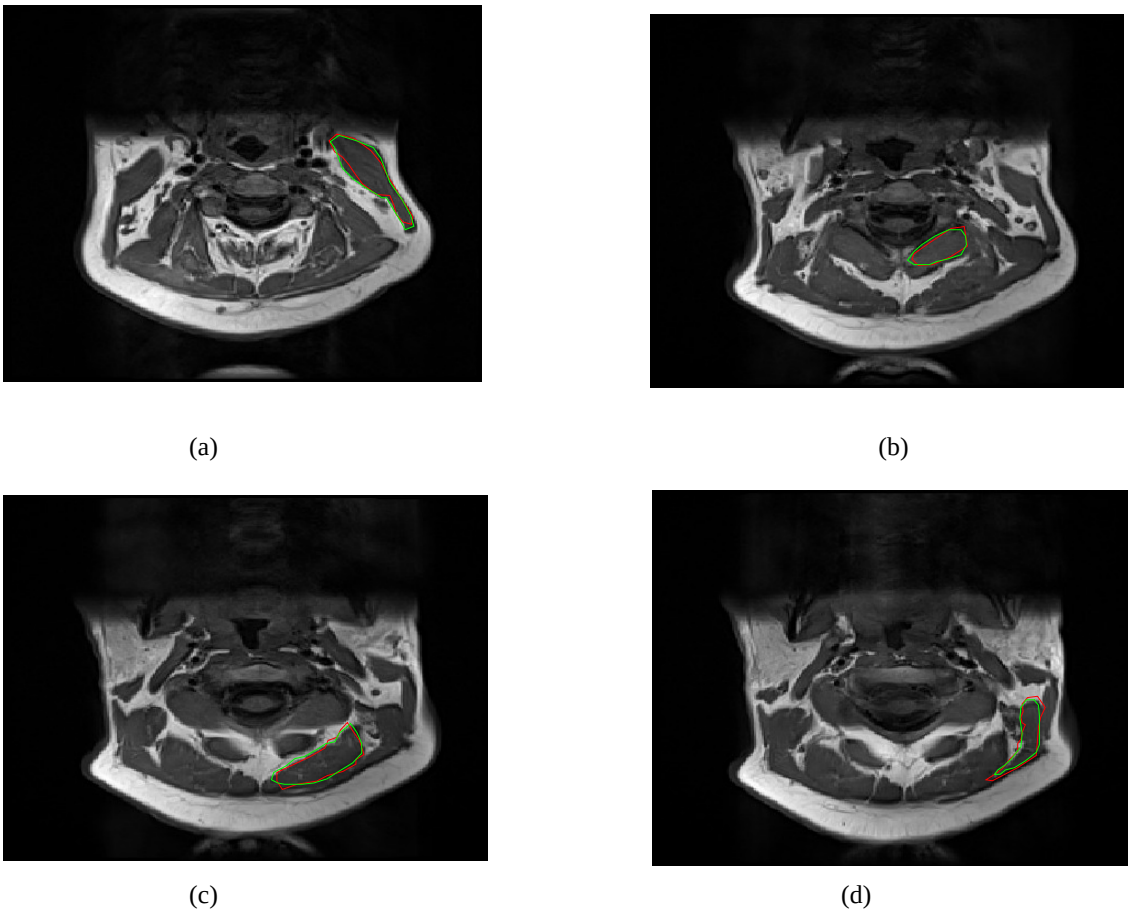

(a) (b) (c) (d)

Figure 1. Segmentation results for (a) right sternocleidomastoid, (b) right obliquus capitus inferior, (c) right semispinalis capitis and (d) right splenius capitis (red curves represent automatic segmentation and green curves manual segmentation).

Method	Muscle Name	DSC
Our method	Neck muscles	0.84±0.0004
Andrews *et al*. [6]	Thigh muscles	0.808±0.074
Ibragimov *et al*. [13]	Tongue muscles	0.81
Gubern *et al*. [11]	Pectoral muscles	0.74
Essafi *et al*. [8]	Calf muscles	0.55
Wang *et al*. [9]	Canine leg muscles	0.78

Table 2. Comparison with other methods for muscle segmentation in terms of mean DSC

4. CONCLUSION AND FUTURE WORK

In this paper, we presented an atlas-based neck muscle segmentation method that used affine and discrete cosine-based elastic registrations. The numerical results showed that our method could be compared favourably with other muscle segmentation methods and our algorithm outperforms in the muscle segmentation paradigm. It obtained a mean DSC of 0.84±0.0004 on real clinical data which indicates good accuracy with consistent segmentation. In future work, our proposed method will be validated on a large set of clinical data using a multi atlas technique to improve segmentation accuracy.

REFERENCES

[1] F. Öhberg, H. Grip, U. Wiklund, Y. Sterner, J. S. Karlsson, and B. Gerdle, "Chronic whiplash associated disorders and neck movement measurements: an instantaneous helical axis approach," *IEEE Transactions on Information Technology in Biomedicine*, vol. 7, no. 4, pp. 274–282, 2003.

[2] L. Barnsley, S. Lord, and N. Bogduk, "Whiplash injury," *Pain*, vol. 58, no. 3, pp. 283–307, 1994.

[3] P-O Bylund and U. Bjornstig, "Sick leave and disability pension among passenger car occupants injured in urban traffic," *Spine*, vol. 23, no. 9, pp. 1023–1028, 1998.

[4] J. M. Elliott, A. R. Pedler, G. A. Jull, L. VanWyk, G. G. Galloway, and S. P. O'Leary, "Differential changes in muscle composition exist in traumatic and nontraumatic neck pain," *Spine*, vol. 39, no. 1, pp. 39–47, 2014.

[5] P-Y Bondiau, G. Malandain, S. Chanalet, P-Y Marcy, J-L Habrand, F Fauchon, P. Paquis, A. Courdi, O. Commowick, I. Rutten, et al., "Atlas-based automatic segmentation of MR images: validation study on the brainstem in radiotherapy context," *International Journal of Radiation Oncology* Biology* Physics*, vol. 61, no. 1, pp. 289–298, 2005.

[6] S. Andrews and G. Hamarneh, "The generalized log-ratio transformation: Learning shape and adjacency prior for simultaneous thigh muscle segmentation," *IEEE Transactions on Medical Imaging*, vol. 34, no. 9, pp. 1773–1787, Sept 2015.

[7] P-Y Baudin, N. Azzabou, P. G. Carlier, and N. Paragios, "Automatic skeletal muscle segmentation through random walks and graph-based seed placement," in *9th IEEE International Symposium on Biomedical Imaging*, 2012, pp. 1036–1039.

[8] S. Essafi, G. Langs, J-F Deux, A. Rahmouni, G. Bassez, and N. Paragios, "Wavelet-driven knowledge-based MRI calf muscle segmentation," in *IEEE International Symposium on Biomedical Imaging,*, 2009, pp. 225-228.

[9] H. Wang, Y. Cao, and T. Syeda-Mahmood, "An experimental study on combining the auto-context model with corrective learning for canine leg muscle segmentation," in *IEEE 12th International Symposium on Biomedical Imaging*, 2015, pp. 1106–1109.

[10] K. Ganesan, U. R. Acharya, K. C. Chua, L. C. Min, and K. T. Abraham, "Pectoral muscle segmentation: a review," *Computer methods and programs in biomedicine*, vol. 110, no. 1, pp. 48–57, 2013.

[11] A. Gubern-Mérida, M. Kallenberg, R. Martí, and N. Karssemeijer, "Segmentation of the pectoral muscle in breast MRI using atlas-based approaches," in *MICCAI*, pp. 371–378. Springer, 2012.

[12] S. M. Kwok, R. Chandrasekhar, Y. Attikiouzel, and M. T. Rickard, "Automatic pectoral muscle segmentation on mediolateral oblique view mammograms," *IEEE Transactions on Medical Imaging*, vol. 23, no. 9, pp. 1129–1140, 2004.

[13] B. Ibragimov, J. L. Prince, E. Z. Murano, J. Woo, M. Stone, B. Likar, F. Pernuˇs, and T. Vrtovec, "Segmentation of tongue muscles from super-resolution magnetic resonance images," *Medical image analysis*, vol. 20, no. 1, pp. 198–207, 2015.

[14] M. N. Aktar,M. J. Alam, andM. Pickering, "A non-rigid 3D multi-modal registration algorithm using partial volume interpolation and the sum of conditional variance," in *International Conference on Digital lmage Computing: Techniques and Applications*, 2014, pp. 1–7.

[15] A. Muhit, M. R. Pickering, M. R. Frater, J. F. Arnold, et al., "Video coding using elastic motion model and larger blocks," *IEEE Transactions on Circuits and Systems for Video Technology*, vol. 20, no. 5, pp. 661–672, 2010.